Liquid Crystals
Publication details, including instructions for authors and subscription information:
http://www.informaworld.com/smpp/title~content=t713926090

Synthesis, structure and characterization of side chain cholesteric liquid crystalline polysiloxanes

Jian-She Hu[a]; Bao-Yan Zhang Corresponding author[a]; Xiao-Zhi He[a]; Chun-Zheng Cheng[a]
[a] The Center for Molecular Science and Engineering, Northeastern University, PR China

Online publication date: 19 May 2010

To cite this Article Hu, Jian-She , Zhang Corresponding author, Bao-Yan , He, Xiao-Zhi and Cheng, Chun-Zheng(2004) 'Synthesis, structure and characterization of side chain cholesteric liquid crystalline polysiloxanes', Liquid Crystals, 31: 10, 1357 — 1365
To link to this Article: DOI: 10.1080/02678290410001718980
URL: http://dx.doi.org/10.1080/02678290410001718980

Liquid Crystals, Vol. 31, No. 10, October 2004, 1357–1365

Synthesis, structure and characterization of side chain cholesteric liquid crystalline polysiloxanes

JIAN-SHE HU, BAO-YAN ZHANG*, XIAO-ZHI HE and CHUN-SHENG CHENG

The Center for Molecular Science and Engineering, Northeastern University, Shenyang 110004, PR China

(*Received 10 August 2003; in final form 31 March 2004; accepted 2 April 2004*)

A series of liquid crystalline homopolysiloxanes and copolysiloxanes were synthesized. The chemical structures of the monomers $\mathbf{M_1}$–$\mathbf{M_7}$ were confirmed by FTIR and ^{1}H NMR spectroscopy. The structure–property relationships of the monomers and polymers are discussed; their phase behaviour and optical properties were investigated by differential scanning calorimetry, thermogravimetric analysis, and polarizing optical microscopy. All the monomers, except $\mathbf{M_2}$ and $\mathbf{M_7}$ showed smectic and nematic phases; the copolymers $\mathbf{P_8}$–$\mathbf{P_{15}}$ displayed cholesteric phases. The homopolymers $\mathbf{P_1}$–$\mathbf{P_7}$ exhibited smectic phases. The selective reflection of cholesteric monomers and copolymers shifted to longer wavelengths with increasing length of the rigid mesogenic core, with decreasing length of the flexible spacer, or with increasing content of nematic units. Experimental results demonstrated that a flexible polymer backbone, a rigid mesogenic core and a long flexible spacer tended to produce a lower glass transition temperature, higher thermal stability, and wider mesophase temperature range.

1. Introduction

In recent years, interest in cholesteric liquid crystalline polymers (ChLCPs) has increased considerably, due to their unique optical properties; these include selective reflection of light, thermochromism and circular dichroism, which final uses in advanced applications such as non-linear optical devices, full colour thermal imaging and organic pigments [1–9]. The cholesteric phase is formed by rod-like, chiral molecules, which, depending on chemical structures, are responsible for the macroscopic alignment of cholesteric domains. Recently, many novel side chain cholesteric LC materials have been reported and their applications explored [10–17]. However, to the best of our knowledge, little detailed research on the relationships between structure and optical properties of ChLCPs has been reported.

In the case of side chain ChLCPs, homopolymers containing cholesteryl mesogenic units usually exhibit smectic phases, although their corresponding monomers show the cholesteric phase. Finkelmann *et al.* reported that ChLCPs were obtained by the copolymerization of two cholesteryl monomers having widely varying flexible spacer length [18]. Side chain ChLCPs were usually prepared by the copolymerization of a nematic monomer and a chiral mesogenic monomer or a chiral non-mesogenic monomer [19, 20].

The aims of our research are: (a) to study structure and optical property relationships of side chain ChLCPs; (b) to supply the necessary data to synthesize more cholesteric LC networks with specific optical properties; (c) to explore the application of ChLCPs in the fields of non-linear optical devices and special coatings. In this study, a series of homopolysiloxanes and copolysiloxanes were synthesized and characterized. Their phase behaviour and optical properties were investigated by differential scanning calorimetry (DSC), thermogravimetric analysis (TGA) and polarizing optical microscopy (POM). The effect of the length of the mesogenic core, flexible spacer and copolymer composition on phase behaviour and optical properties is discussed.

2. Experimental

2.1. *Materials*

Polymethylhydrosiloxane (PMHS, $\overline{M}_n = 700$–800) was purchased from Jilin Chemical Industry Co, 4-hydroxybiphenyl-4′-carboxylic acid from Aldrich, and cholesterol from Henan Xiayi Medical Co. Hexachloroplatinate(IV) catalyst was obtained from Shenyang Chemical Reagent Co. Toluene used in the

*Author for correspondence;
e-mail: baoyanzhang@hotmail.com

Liquid Crystals ISSN 0267-8292 print/ISSN 1366-5855 online © 2004 Taylor & Francis Ltd
http://www.tandf.co.uk/journals
DOI: 10.1080/02678290410001718980

hydrosilylation reaction was first heated at reflux over sodium and then distilled under nitrogen. All other solvents and reagents were purified by standard methods.

2.2. *Characterization*

FTIR spectra were measured on a Nicolet 510 FTIR spectrometer. ^{1}H NMR spectra (300 MHz) were recorded on a Varian WH-90PFT spectrometer. The phase transition temperatures and thermodynamic parameters were determined using a Perkin-Elmer DSC-7 equipped with a liquid nitrogen cooling system. Heating and cooling rates were $10^\circ C\,min^{-1}$. The phase transition temperatures were noted during the second heating and first cooling scans. The thermal stability of the polymers was measured with a Perkin-Elmer TGA-7 thermogravimetric analyser using a $20^\circ C\,min^{-1}$ heating rate. A Leitz Microphot-FX polarizing optical microscope equipped with a Mettler FP 82 hot stage and FP 80 central processor, was used to observe phase transition temperatures and analyse mesomorphic properties for LC monomers and polymers through observation of optical texture.

2.3. *Monomers synthesis*

The synthetic route to the olefinic monomers is shown in scheme 1. The yields and structural characterization of the monomers are shown in table 1. Cholesteryl acrylate (**M$_1$**), cholesteryl allylether (**M$_2$**), cholesteryl 4-allyloxybenzoate (**M$_3$**), cholesteryl

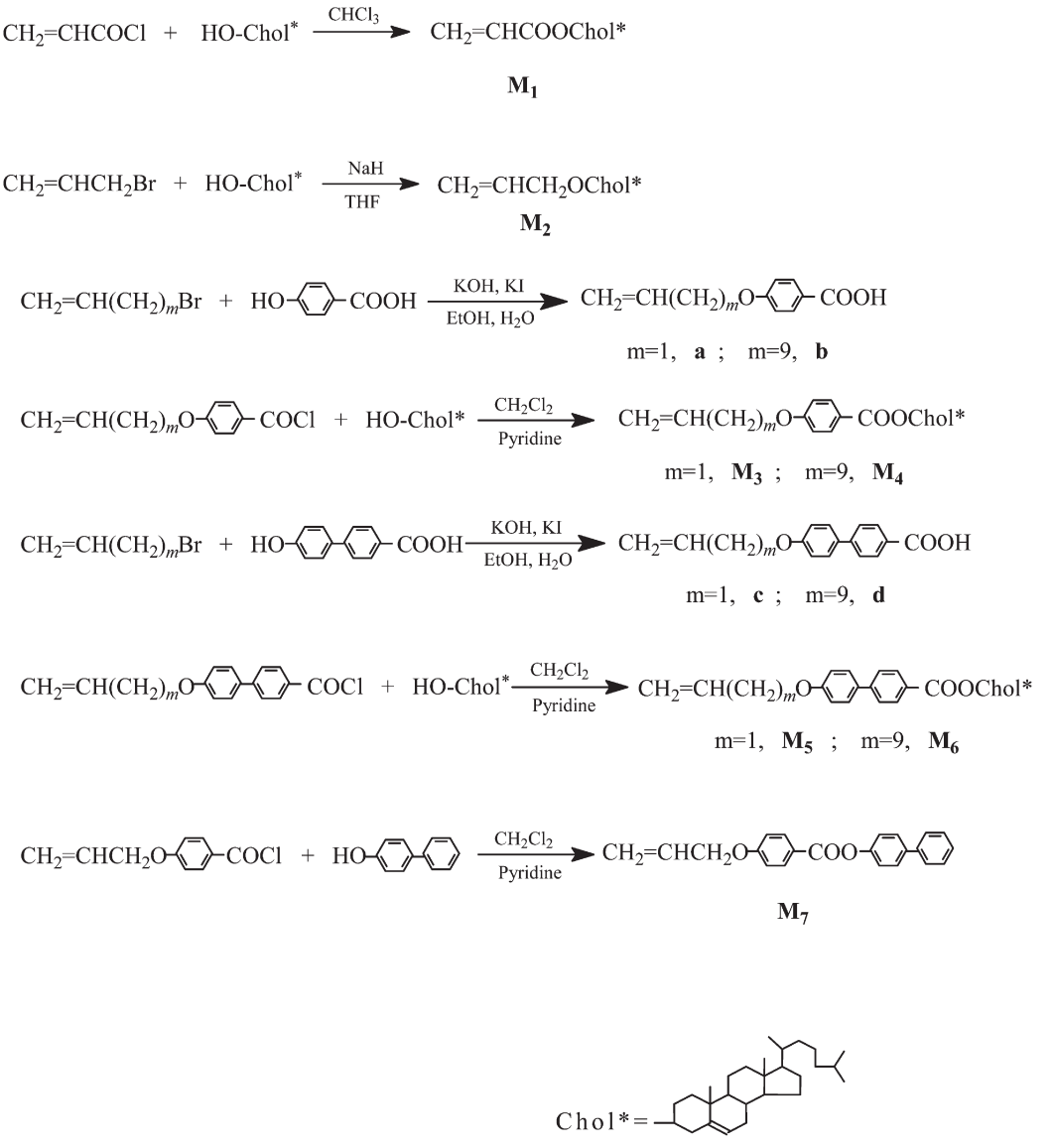

Scheme 1. Synthesis of liquid crystalline monomers.

Table 1. Yields and characterization of monomers.

Monomer	*m*	Yield/%	IR (KBr)/cm^{-1}	^1H NMR chemical shifts ($CDCl_3$, δ/ppm)
M_1	—	72	3073 (=CH), 2940, 2850 (CH_3, CH_2), 1723 (C=O), 1635(C=C)	0.68–1.99 (m, 43H); 3.78 (t, 2H); 5.48 (m, 2H); 6.17 (m, 1H)
M_2	—	47	3081 (=CH), 2960, 2856 (CH_3, CH_2), 1631 (C=C)	0.65–1.92 (m, 43H); 4.62 (t, 2H); 5.43 (m, 2H); 6.06 (m, 1H)
M_3	1	70	3051 (=CH), 2965, 2854 (CH_3, CH_2), 1735 (C=O), 1634 (C=C), 1606, 1508 (Ar)	0.67–2.03 (m, 43H); 4.47 (t, 2H); 4.69–5.18 (m, 2H); 5.36 (m, 1H); 6.02 (m, 1H); 6.92–7.98 (m, 4H)
M_4	9	58	3076 (=CH), 2961, 2859 (CH_3, CH_2), 1733 (C=O), 1645 (C=C), 1605, 1510 (Ar)	0.62–2.15 (m, 57H); 2.41 (d, 2H); 3.96 (t, 2H); 4.83–5.11 (m, 3H); 5.39 (m, 1H); 5.93 (m, 1H); 6.90–8.03 (m, 4H)
M_5	1	63	3063 (=CH), 2930, 2852 (CH_3, CH_2), 1741 (C=O), 1636 (C=C), 1606, 1512 (Ar)	0.66–2.07 (m, 43H); 4.55 (t, 2H); 4.72–5.29 (m, 2H); 5.51 (m, 1H); 6.04 (m, 1H); 7.03–8.06 (m, 8H)
M_6	9	44	3061 (=CH), 2927, 2853 (CH_3, CH_2), 1737 (C=O), 1640 (C=C), 1603, 1504 (Ar)	0.65–2.14 (m, 57H); 2.43 (d, 2H); 4.07 (t, 2H); 4.81–5.08 (m, 3H); 5.42 (m, 1H); 5.81 (m, 1H); 6.96–8.12 (m, 8H)
M_7	—	53	3039 (=CH), 2963, 2849 (CH_3, CH_2), 1731 (C=O), 1636 (C=C), 1610, 1512 (Ar)	4.60 (t, 2H); 5.51 (m, 2H); 6.04 (m, 9H)

4-(undec-10-en-1-yloxy)benzoate (**M_4**), cholesteryl 4-allyloxybiphenyl-4′-carboxylate (**M_5**), cholesteryl 4-(undec-10-en-1-yloxy)biphenyl-4′-carboxylate (**M_6**), and 4-biphenyl-4′-allyloxybenzoate (**M_7**) were synthesized according to the reported literature [16, 21–25].

2.4. *Polymers synthesis*

The synthesis of the homopolysiloxanes **P_1**–**P_7** and copolysiloxanes **P_8**–**P_{15}** is shown in schemes 2 and 3, respectively. **P_1**–**P_{15}** were synthesized by equivalent methods. For the representative synthesis of **P_{10}**, the monomers **M_3**, **M_7**, and PMHS were dissolved in toluene. The reaction mixture was heated to 65°C under nitrogen, and then 2 ml of THF solution of hexachloroplatinate(IV) catalyst (5 mg ml^{-1}) was injected with a syringe. The progress of the hydrosilication reaction, monitored from the Si–H stretch intensity, went to completion within 30 h as indicated by IR. The polymers were obtained by precipitation with methanol, and then dried under vacuum. IR (KBr): 2953–2843 (–CH_3, –CH_2–); 1736 (C=O); 1608, 1512 (Ar–); 1300–1000 cm^{-1} (Si–O–Si, C–Si and C–O–C).

3. Results and discussion

3.1. *Phase behaviour*

The phase behaviour of side chain LCPs depends on the nature of the polymer backbone, the length of the mesogenic core, the flexible spacer, and the copolymer composition. The mesogens are usually attached to the polymer backbone through the flexible spacer. The polymer backbone and mesogens have antagonistic tendencies: the polymer backbone is driven towards a random coil-type configuration, whereas the mesogens stabilize with long range orientational order. The flexible spacer, which is general an aliphatic hydrocarbon chain containing, normally, more than two methylene units, decouples the mesogenic side groups from the polymer backbone and renders the mesogens to orientational-order.

The phase transition temperatures and corresponding enthalpy changes of monomers **M_1**–**M_7** and polymers **P_1**–**P_{15}**, obtained on the second heating and the first cooling scan, are summarized in tables 2, 3, and 4. All phase transitions were reversible and did not change on repeated heating and cooling cycles. The phase transition temperatures determined by DSC were consistent with POM results.

As seen from the data listed in table 2, molecular structures had a considerable effect on phase transition temperatures of **M_1**–**M_6**. Compared with the melting temperature (T_m) and the clearing temperature (T_i) of **M_2**, T_m of **M_3** and **M_5** increased by 25.6 and 29.0°C, and T_i increased to 223.7 and 251.7°C with increasing length of mesogenic core. With an increase in the length of the flexible spacer, T_m and T_i of **M_4** decreased by 41.0 and 21.8°C over those of **M_3**, and T_m and T_i of **M_6**

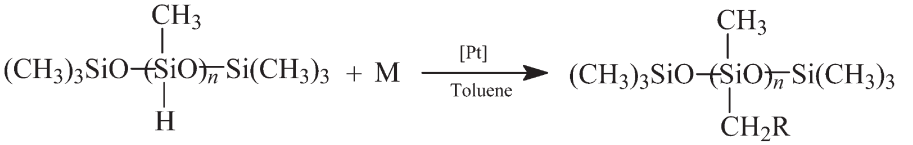

P_1, R = $-CH_2COOChol^*$

P_2, R = $-CH_2CH_2OChol^*$

P_3, R = $-CH_2CH_2O-C_6H_4-COOChol^*$

P_4, R = $-CH_2(CH_2)_9O-C_6H_4-COOChol^*$

P_5, R = $-CH_2CH_2O-C_6H_4-C_6H_4-COOChol^*$

P_6, R = $-CH_2(CH_2)_9O-C_6H_4-C_6H_4-COOChol^*$

P_7, R = $-CH_2CH_2O-C_6H_4-COO-C_6H_4-C_6H_5$

Scheme 2. Synthesis of homopolysiloxanes.

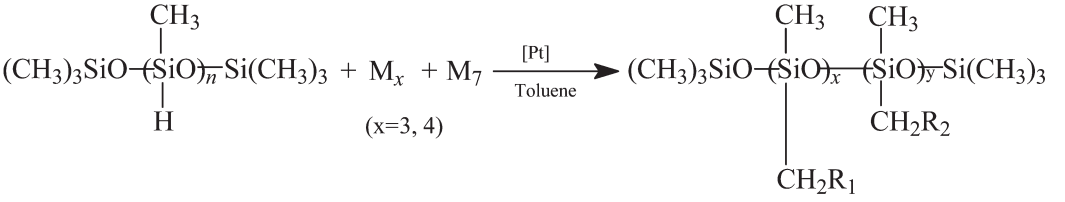

$R_1 = -CH_2CH_2O-C_6H_4-COOChol^*$

$R_2 = -CH_2CH_2O-C_6H_4-COO-C_6H_4-C_6H_5$

$P_8 - P_{11}$

$R_1 = -CH_2(CH_2)_9O-C_6H_4-COOChol^*$

$R_2 = -CH_2CH_2O-C_6H_4-COO-C_6H_4-C_6H_5$

$P_{12} - P_{15}$

Scheme 3. Synthesis of copolysiloxanes.

decreased by 39.7 and 10.4°C over those of **M_5**. However, because T_i decreased less than T_m, the mesophase temperature ranges (ΔT) of **M_4** and **M_6** widened by 19.2 and 29.3°C in comparison with those of corresponding **M_3** and **M_5**.

As with the monomers, chemical structure also affected the phase behaviour of **P_2**–**P_6**. From table 3, in comparison with the glass transition temperature (T_g) and T_i of **P_2**, with increasing length of mesogenic core, the T_g of **P_3** and **P_5** increased by 30.7 and 32.8°C, respectively; T_i increased by 128.3 and 164.7°C, and ΔT widened by 97.6 and 131.9°C because T_i increased more than T_g. With increasing spacer length, T_g and T_i of **P_4** decreased by 52.6 and 23.5°C over those of **P_3**; and T_g and T_i of **P_6** decreased by 50.9 and 18.2°C over those of **P_5**. However, because T_i decreased less than T_g, ΔT of **P_4** and **P_6** widened by 29.1 and 32.7°C, respectively, over those of corresponding **P_3** and **P_5**. These

Table 2. Phase transition temperatures of monomers. Cr = solid, Ch = cholesteric, SmA = smectic A, N = nematic, I = isotropic; peak temperatures were taken as phase transition temperatures.

Monomer	m	Transition temperature/°C (Corresponding enthalpy changes/J g^{-1}) Heating / Cooling	ΔT
M$_1$	—	Cr79.6(48.8)Ch124.3(1.3)I / I119.1(0.9)Ch25.5(10.3)Cr	44.7
M$_2$	—	Cr82.6(50.2)I / I80.5(1.4)SmA70.2(36.3)Cr	—
M$_3$	1	Cr108.2(42.5)Ch223.7(1.6)I / I215.7(1.1)Ch74.5(31.3)Cr	115.5
M$_4$	9	Cr67.2(35.1)Ch201.9(0.9)I / I197.8(0.7)Ch35.6(33.2)Cr	134.7
M$_5$	1	Cr111.6(50.6)Ch251.7(1.8)I / I234.2(1.3)Ch81.5(39.7)Cr	140.1
M$_6$	9	Cr71.9(41.4)Ch241.3(1.4)I / I227.5(0.9)Ch32.2(42.4)Cr	169.4
M$_7$	—	Cr134.8(34.4)I / I132.4(1.3)N101.9(28.7)Cr	—

Mesophase temperature ranges on heating.

Table 3. Thermal properties of homopolysiloxanes.

Polymer	T_g/°C	T_i/°C	ΔH_i/J g^{-1}	ΔT[a]	LC phase	T_d[b]/°C
P$_1$	84.2	—	—	—	—	328.6
P$_2$	32.6	147.8	4.2	115.2	SmA	301.5
P$_3$	63.3	276.1	3.3	212.8	SmA	331.3
P$_4$	10.7	252.6	1.7	241.9	SmA	317.7
P$_5$	65.4	312.5	2.8	247.1	SmA	348.9
P$_6$	14.5	294.3	2.1	279.8	SmA	334.6
P$_7$	64.6	176.1	1.1	111.5	N	306.1

[a] Mesophase temperature ranges (T_i–T_g).
[b] Temperature at which 5% weight loss occurred.

Table 4. Thermal properties of copolysiloxanes.

Polymer	R_1/R_2[a]	T_g/°C	T_i/°C	ΔH_i/J g^{-1}	ΔT[b]	LC phase	λ_m[c]/nm
P$_8$	90/10	63.0	267.2	1.2	204.2	Ch	1109
P$_9$	80/20	64.3	262.1	1.5	197.8	Ch	1132
P$_{10}$	70/30	63.5	249.8	0.9	186.3	Ch	1168
P$_{11}$	50/50	64.2	221.3	1.3	157.1	Ch	1296
P$_{12}$	90/10	17.6	240.3	1.2	222.7	Ch	952
P$_{13}$	80/20	30.4	231.5	1.1	201.1	Ch	961
P$_{14}$	70/30	32.5	214.8	1.4	182.3	Ch	986
P$_{15}$	50/50	43.7	210.6	1.0	166.9	Ch	1139

[a] Initial mole ratio of cholesteric and nematic monomers.
[b] Mesophase temperature ranges (T_i–T_g).
[c] Reflection wavelength measured by UV/vis spectroscopy in the cholesteric phase.

phenomena are explained as follows: when the phenyl ring is introduced into the mesogenic molecule, the length of the mesogenic core increases, and the intermolecular force is enhanced, causing an increase in the T_g, T_m and T_i; with an increase of the spacer length, the molecular flexibility increases, causing a decrease in T_g, T_m and T_i.

In addition, copolymer composition can also affect the phase behavior of LCPs. Figures 1 and 2 illustrate the influence of copolymer composition on the phase behaviour of the copolymers. With increasing content of nematic units, T_g of **P$_8$**–**P$_{11}$** hardly changed and T_i clearly decreased; T_g of **P$_{12}$**–**P$_{15}$** increased and T_i decreased.

TGA results showed that the temperatures at which

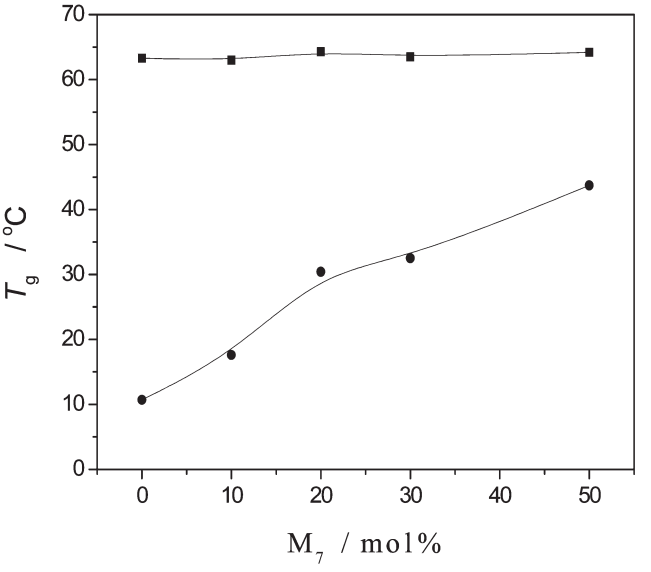

Figure 1. Effect of **M$_7$** concentration on T_g of copolymers: ■ **P$_8$**–**P$_{11}$**; ● **P$_{12}$**–**P$_{15}$**.

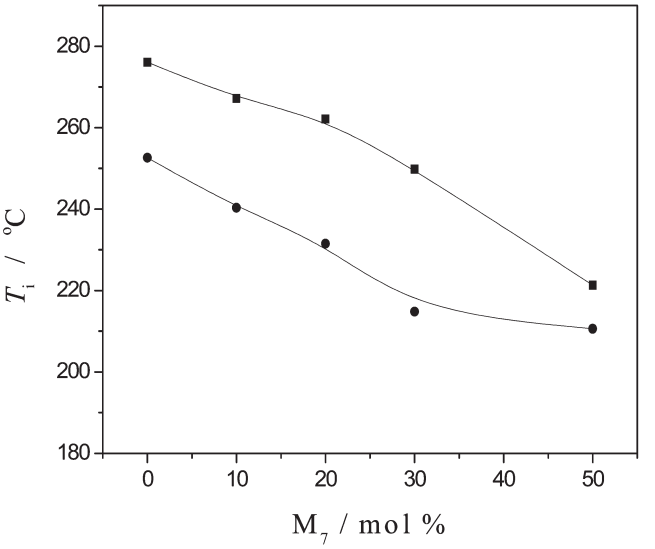

Figure 2. Effect of **M$_7$** concentration on T_i of copolymers: ■ **P$_8$**–**P$_{11}$**; ● **P$_{12}$**–**P$_{15}$**.

5% weight loss occurred (T_d) were greater than 300°C for $\mathbf{P_1}$–$\mathbf{P_7}$, showing that the synthesized side chain LC polysiloxanes have a higher thermal stability.

In a comparison of phase transition temperatures of the polymers, it can be seen that a flexible polymer backbone, a rigid mesogenic core and a long flexible spacer tend toward a low glass transition temperature, high thermal stability, and a wide mesophase temperature range. The most important tendency was that the flexible polymer backbone encouraged a wide mesophase temperature range [24–27].

3.2. *Optical properties*

The unique optical properties of ChLCPs are related to the helical supermolecular structure of the cholesteric phase. The periodic helical structure of the cholesteric phase selectively reflects visible light like a diffraction grating, whose pitch controls the wavelength of selective reflection of light. If the reflected wavelength lies in the visible range of the spectrum, the cholesteric phase exhibits brilliant colours. The transmitted light shows a complementary colour. The wavelength of selective reflection of light λ_m obeys the Bragg condition:

$$\lambda_m = \bar{n}P \tag{1}$$

where $\bar{n}$ is the average index of refraction, and P is the pitch of the cholesteric phase, defined as the spatial distance over which the director rotates 360°.

Due to the angular dependence of the reflection conditions, different colours are seen depending on different observation angles. So λ_m is given by

$$\lambda_m = \bar{n}P\cos\theta \tag{2}$$

where θ is the angle of incidence. When $\theta = 0°$ (normal incidence), $\lambda_m = \lambda_0 = \bar{n}P$. The intensity of reflected light is a maximun at $\lambda_m = \lambda_0$, and falls off very rapidly on either side of λ_0 [28].

In reality, the orientation of the cholesteric helices is not exactly perpendicular to the cell surface. Taking this into account, equation (2) becomes

$$\lambda_m = \bar{n}P\cos\left\{\frac{1}{2}\left[\sin^{-1}\left(\frac{\sin\alpha}{\bar{n}}\right) + \sin^{-1}\left(\frac{\sin\beta}{\bar{n}}\right)\right]\right\} \tag{3}$$

where α and β are the incidence angle and observation angle, respectively, [29].

The helical pitch is an important parameter in connection with structures and optical properties of the cholesteric phase. Although the microscopic origins of the helical pitch are still a subject of study [30], it is known that the pitch and the reflection wavelength depend on the molecular structure, such as the polymer backbone, the length of mesogenic core, flexible spacer length, copolymer composition, and external conditions (e.g. temperature, intermolecular force, electric, and magnetic field). The lengths of mesogenic core and flexible spacer affect not only the phase transition temperatures, but also the selective reflection wavelength of the cholesteric phase. For $\mathbf{M_1}$ and $\mathbf{M_3}$–$\mathbf{M_6}$, the selective reflection of light shifted to the long wavelength region with increasing length of mesogenic core or decreasing length of flexible spacer.

In Figure 3 the inverse reflection wavelength λ_m^{-1} of copolymer films is plotted against the mole fraction of cholesteric monomer. The effect of the content of cholesteric monomer on the reflection wavelength is described by the helical twisting power (*HTP*), which is defined as the initial slope of the inverse helical pitch P^{-1} vs. the mole fraction χ_{ch} of the chiral dopant.

$$HTP = \left(\frac{dP^{-1}}{d\chi_{ch}}\right)_T = \bar{n}\left(\frac{d\lambda_m^{-1}}{d\chi_{ch}}\right)_T. \tag{4}$$

This equation has been developed for mixtures of chiral guest molecules in a low molar mass nematic host [31]. Later it was shown to be valid also for cholesteric copolymers [32]. According to figure 3, the curve of λ_m^{-1} vs the mole fraction of cholesteric monomer tends to flatten when the content of cholesteric monomer increases from 50 to 90 mol%, which is consistent with results reported for cholesteric copolymers [33, 34]. That is, the selective reflection of cholesteric copolymers also shifts to the long wavelength region with increasing content of nematic units.

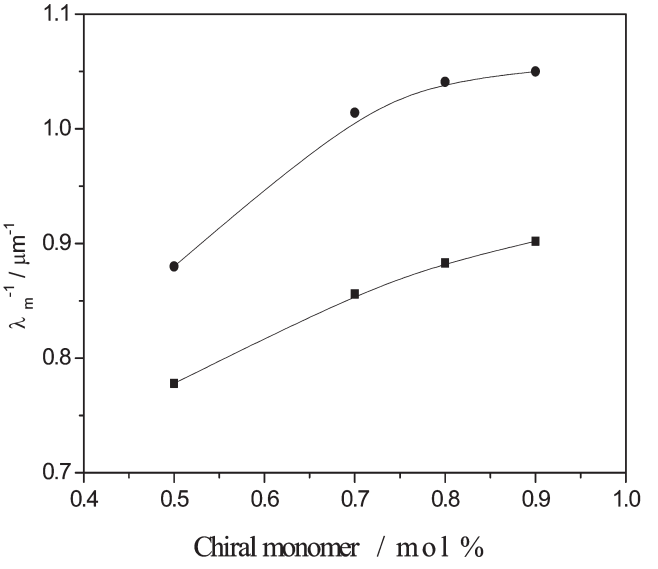

Figure 3. λ_m^{-1} as a function of the mole fraction of chiral monomer in the copolymers: ■ $\mathbf{P_8}$–$\mathbf{P_{11}}$; ● $\mathbf{P_{12}}$–$\mathbf{P_{15}}$.

Moreover, the selective reflection of the cholesteric phase shifted to the short wavelength region with increasing temperature, so λ_m was temperature-dependent. According to equation (2), an increase of the observation angle (reflection angle) shifted the selective reflection of light to the short wavelength region. In addition, planar and focal-conic textures can also interchange under electric and magnetic fields, as described in detail by Meyer [35] and de Gennes [36].

In addition, the helical pitch not only affects the selective reflection wavelength and colour, but is also related to texture type of the cholesteric phase. In general, a cholesteric LC at zero field exhibits two optically contrasting stable states: planar (including oily-streak and Grandjean) and focal-conic textures. When the cholesteric phase is in the planar texture, the helical axis is perpendicular to the cell surface, and the material Bragg-reflects coloured light; when the cholesteric phase is in the focal-conic texture, the helical axis is more or less parallel to the cell surface, the material is forward-scattering and no selective light reflection appears.

POM results showed that the monomers **M1** and **M3**–**M6** exhibit enantiotropic cholesteric oily-streak texture and focal-conic texture during heating or cooling. When these cholesteric monomers were heated to melting temperature, an obvious oily-streak texture appeared and except for **M5**, a reflection colour was observed. On cooling the samples from the isotropic melt, a focal-conic texture was formed, which was easily transformed into oily-steak texture by shearing the mesophase. Photomicrographs of **M1** and **M3** are shown as examples in figures 4 (*a*) and 4 (*b*). **M2** and **M7** exhibited monotropic mesomorphism, and showed, respectively, smectic fan-shaped and nematic threaded textures during cooling. In contrast to **M3**–**M6**, **M2** did not display the expected cholesteric phase although this monomer also contained the cholesteryl group. This is because the molecular transverse attractive force is greater than the terminal attractive force, preventing the formation of a helical structure.

The homopolymer **P1** showed no texture because of its shorter spacer length and the greater steric hindrance of the bulky cholesteryl group, which disturbed the orientation of the mesogenic groups. **P2**–**P6** exhibited enantiotropic smectic fan-shaped textures, but the expected cholesteric phase did not occur. This is because the polymeric chains hinder the formation of a helical supermolecular mesogenic structure, and the mesogenic moieties are ordered in a smectic orientation with their centres of gravity in planes. **P7** displayed a nematic threaded texture. The copolymers **P8**–**P15** exhibited cholesteric oily-streak texture or Grandjean texture on heating and cooling,

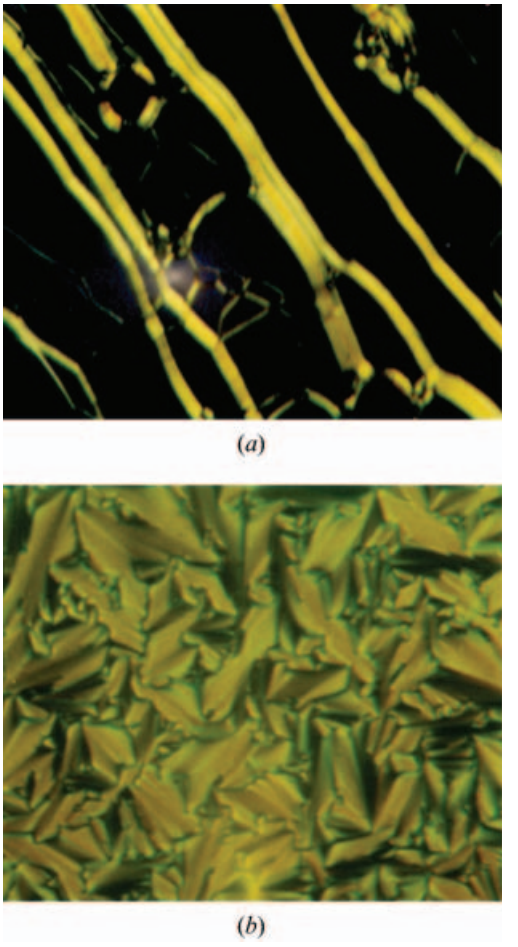

Figure 4. Optical textures of monomers (320×): (*a*) oily-streak texture of **M1** at 116°C; (*b*) focal-conic texture of **M3** at 211°C.

but no selective reflection properties were observed, because the reflection wavelength was greater than the wavelength of visible light. Photomicrographs of **P5**, **P10** and **P14** are shown in figures 5 (*a*–*c*).

4. Conclusions

LC monomers **M1**–**M7**, homopolysiloxanes **P1**–**P7**, and copolysiloxanes **P8**–**P15** were prepared and characterized. **M1** and **M3**–**M6** exhibited cholesteric oily-streak texture and focal-conic texture. **M2** and **M7**, respectively, displayed smectic fan-shaped texture and nematic threaded texture only during cooling. **P2**–**P6** showed smectic phases, **P7** showed a nematic phase and **P8**–**P15** showed cholesteric phases. All of the polymers obtained displayed very wide mesophase temperature ranges. The selective reflection of cholesteric monomers and copolysiloxanes shifted to longer wavelengths with increasing length of mesogenic core or reducing length of flexible spacer. In addition, the selective reflection of

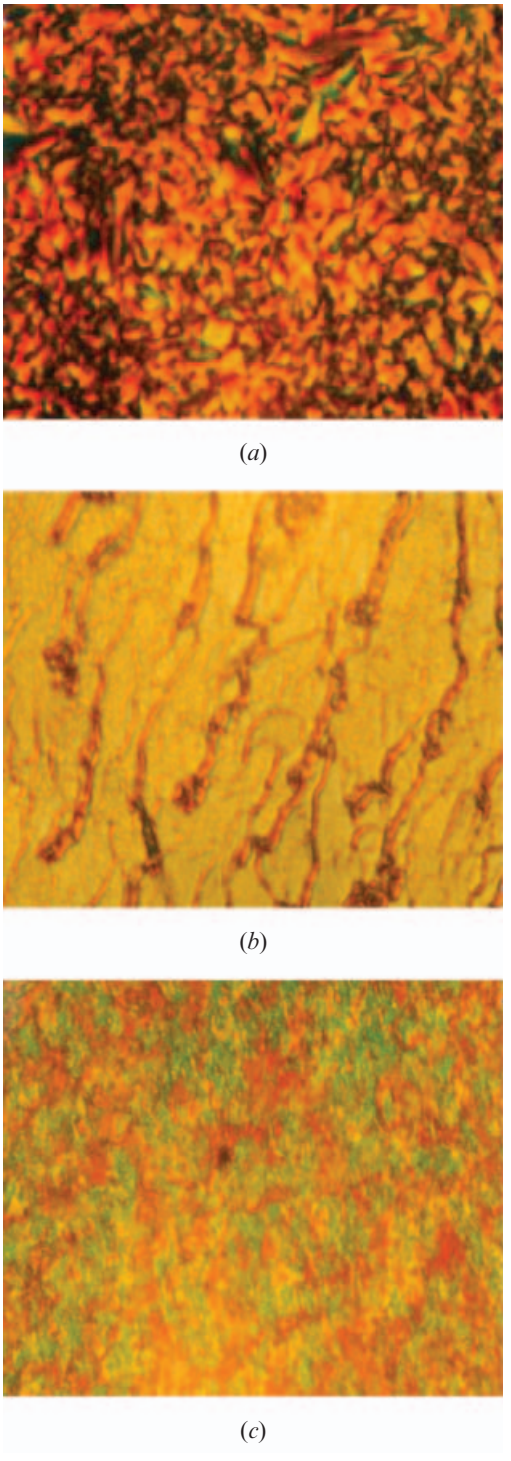

(*a*)

(*b*)

(*c*)

Figure 5. Optical textures of polymers (320×): (*a*) fan-shaped texture of $\mathbf{P_5}$ at 245°C; (*b*) oily-streak texture of $\mathbf{P_{10}}$ at 223°C; (*c*) Grandjean texture of $\mathbf{P_{14}}$ at 191°C.

the copolymers shifted to shorter wavelengths with increasing content of chiral units. A flexible polymer backbone, a rigid mesogenic core and a long flexible spacer tended to lead to a lower glass transition temperature, higher thermal stability, and wider mesophase temperature range.

The authors are grateful to the *National Natural Science Fundamental Committee of China, HI-Tech Research and Development Program (863) of China, the Science and Technology Research Major Project of the Ministry of Education of China, and the Science and Technology Bureau of Shenyang* for financial support.

References

[1] Mcdonell, D. G., 1987, in *Thermotropic Liquid Crystals*, edited by G. W. Gray (New York: John Wiley), p. 120.
[2] Belayev, S. V., Schadt, M. I., Funfschiling, J., Malimoneko, N. V., and Schmitt, K., 1990, *Jpn. J. appl. Phys.*, **29,** L634.
[3] Broer, D. J., Lub, J., and Mol, G. N., 1995, *Nature*, **378,** 467.
[4] Bunning, T. J., and Kreuzer, F. H., 1995, *Trends polym. Sci.*, **3,** 318.
[5] Yang, D. K., West, J. L., Chien, L. C., and Doane, J. W., 1994, *J. appl. Phys.*, **76,** 1331.
[6] Kricheldorf, H. R., Sun, S. J., and Chen, C. P., 1997, *J. polym. Sci. A: polym. Chem.*, **35,** 1611.
[7] Peter, P. M., 1998, *Nature*, **391,** 745.
[8] Sapich, B., Stumpe, J., and Kricheldorf, H. R., 1998, *Macromolecules*, **31,** 1016.
[9] Sun, S. J., Liao, L. C., and Chang, T. C., 2000, *J. polym. Sci. A: polym. Chem.*, **38,** 1852.
[10] Stohr, A., and Strohriegl, P., 1998, *Macromol. Chem. Phys.*, **199,** 751.
[11] Dierking, I., Kosbar, L. L., and Held, G. A., 1998, *Liq. Cryst.*, **24,** 387.
[12] Pfeuffer, T., and Strohriegl, P., 1999, *Macromol. Chem. Phys.*, **200,** 2480.
[13] Espinosa, M. A., Cadiz, V., and Galia, M., 2001, *J. polym. Sci. A: polym. Chem.*, **39,** 2847.
[14] Hu, J. S., Zhang, B. Y., Sun, K., and Li, Q. Y., 2003, *Liq. Cryst.*, **30,** 1267.
[15] Zhang, B. Y., Hu, J. S., Jia, Y. G., and Du, B. G., 2003, *Macromol. Chem. Phys.*, **204,** 2123.
[16] Hu, J. S., Zhang, B. Y., Jia, Y. G., and Chen, S., 2003, *Macromolecules*, **36,** 9060.
[17] Zhang, B. Y., Hu, J. S., Wang, Y., and Qian, J. H., 2003, *Polym. J.*, **35,** 476.
[18] Finkelmann, H., Ringsdorf, H., Siol, W., and Wendorff, H., 1978, *Makcromol. Chem.*, **179,** 829.
[19] Finkelmann, H., Koldehoff, J., and Ringsdorf, H., 1978, *Angew. Chem. int. Ed. Engl.*, **17,** 935.
[20] Mihaea, T., Nozuhiro, K., Funaki, K., and Koide, N., 1997, *Polym. J.*, **29,** 309.
[21] Janini, G. M., Laub, R. J., and Shaw, T. J., 1985, *Macromol. Chem. rapid. Commun.*, **6,** 57.
[22] Adams, N. W., Bradshaw, J. S., Bayona, J. M., Markides, K. E., and Lee, M. L., 1987, *Mol. Cryst. liq. Cryst.*, **147,** 43.
[23] Lin, J. L., and Hsu, C. S., 1993, *Polym. J.*, **25,** 153.
[24] Lin, C. H., and Hsu, C. S., 2000, *Polym. Bull.*, **45,** 53.
[25] Hu, J. S., Zhang, B. Y., Liu, L. M., and Meng, F. B., 2003, *J. appl. polym. Sci.*, **89,** 3944.

[26] HSU, C. S., LIN, J. L., CHOU, L. R., and HSIUE, G. H., 1992, *Macromolecules*, **25,** 7126.
[27] HU, J. S., ZHANG, B. Y., FENG, Z. L., and WANG, H. G., 2001, *J. appl. polym. Sci.*, **80,** 2335.
[28] DAS, P., XU, J., and ROY, J., 1999, *J. chem. Phys.*, **111,** 8240.
[29] EBERLE, H. T., MILLER, A., and KREUZER, F. H., 1989, *Liq. Cryst.*, **5,** 907.
[30] HARRIS, A. B., KAMIEN, R. D., and LUBENSKY, T. C., 1997, *Phys. Rev. Lett.*, **78,** 1476.
[31] FINKELMANN, H., and STEGEMEYER, G., 1978, *Ber. Bunsenges Phys. Chem.*, **82,** 1302.
[32] FINKELMANN, H., and REHAGE, G., 1980, *Makcromol. Chem. rapid. Commun.*, **1,** 733.
[33] FINKELMANN, H., and REHAGE, G., 1984, *Adv. polym. Sci.*, **60/61,** 99.
[34] SHIBAEV, V. P., and PLATE, N. A., 1984, *Adv. polym. Sci.*, **60/61,** 273.
[35] MEYER, R. B., 1968, *Appl. Phys. Lett.*, **12,** 281.
[36] DE GENNES, P. G., 1968, *Solid State Commun.*, **6,** 163.